Multi-Regime CFD Optimization of Diverter-less Supersonic Intake Bump Geometry for Enhanced Engine Pressure Recovery

Muhammad Ali[1], Haroon Saqlain Khan[2], Mudasir Ghafoor[3], and Saad Mujtaba[4]

[1] Graduate Researcher, Department of Mechanical and Materials Engineering, Western University, Canada
[2] Graduate Researcher, Department of Materials Engineering, School of Chemicals & Materials Engineering, National, University of Science & Technology, Pakistan.
[3] Graduate Researcher, Department of Aerospace, College of Aeronautical Engineering (CAE), National University of Science & Technology, Pakistan.
[4] Independent Researcher, Aerospace Engineering, Istanbul, Turkey

Correspondence should be addressed to Muhammad Ali   Malik.ali@gmail.com

ABSTRACT- Aircraft intake plays a vital role in overall performance of the aircraft. Purpose of intake is to supply less turbulent and smooth flow to the engine. It must provide maximum pressure recovery for a wide range of operating conditions. Conventional ramp intakes have been used in many older and few modern fighter aircraft (F4 Phantom II, Mig 21, Mig 27, Mirage 2000 & F-14 Tomcat). However, DSI (Diverter Less Supersonic Intake) were used in modern aircraft (JF -17 Block 3, F- 35 & J - 20). Weight, complexity & maintenance cost can be reduced using DSI compared in comparison to the conventional intake. Furthermore, DSI provides higher pressure recovery, lesser boundary layer & less complex geometry. The aim of this research is to model different bump configurations and carry out their CFD analysis in order to establish high performing configuration of DSI air intakes at subsonic & supersonic regimes. Four bump configurations named as smaller, softer, blunter and original bump were modelled in ANSYS at three different speed regimes (Mach No 0.6, 0.95 & 1.5) & comparison was drawn for each type of DSI bump configuration & it was found that pressure recovery of DSI of all four configuration is approximately same in subsonic regions whereas for transonic regime (Mach 0.95) DSI smaller has highest pressure recovery value of 0.868 & supersonic regime bump original has highest pressure recovery value of 0.779. This shows that smaller & smoother bump intake configuration will provide maximum pressure recovery and its position into the air intake is crucial for the pressure recovery.

KEYWORDS- CFD, Supersonic Intake, Bump Geometry, Engine Pressure Recovery

I. INTRODUCTION

Primary function of the air intakes is to ensure smooth flow to the engine despite of air approaching the aircraft from direction other than straight ahead. Normally the design point of the compressor is set at about half of the speed of sound (M=0.5) hence the flow has to accelerate at flight speed lower than this (M<0.5) to match the design point. In the very same way flow has to decelerates at flight speed higher than the design point (M>0.5). Due to these reasons the internal profile of the inlet duct has to accommodate both accelerating and decelerating flows without any undue losses. [1]. The design of subsonic inlet duct is somewhat easier than supersonic aircraft. The reason is that in subsonic aircraft, the inlet faces only subsonic regime and the phenomenon of shock waves and distortion are neglected completely. The design of the supersonic inlet is quite complex and time consuming keeping in view the concept of shock waves generation. In supersonic aircraft, the inlets have different features which exploit the process of shock wave generation to slow down the flow velocity. The air slows down from supersonic to subsonic through shock waves and then from subsonic to engine design point through the inlet duct (Diffuser). A particular system of inlet is chosen keeping in view different constraint such as type of aircraft, cost, time, and operational needs to minimize frictional and shockwaves losses which in turn maximizes the pressure recovery at the compressor. A good intake design is characterized by providing high pressure recovery and low distortion. Therefore, it is essential to divert as much of the boundary layer as possible since it is a factor which affect the quality of the airflow. Pressure recovery is defined as the ratio of total pressure at the engine face and intake face. In other words, it is the average total pressure at the engine face, Aerodynamic Interface Plane (AIP) divided by the free stream total pressure. For engines that are integrated with the body, for example on fighter aircraft, the airflow is travelling along the body of the aircraft before it reaches the air intake. A boundary layer builds up along the body which is not desirable, especially in the part of the flow that supplies the engines. Thus, in order to reduce the boundary layer thickness of air flow intake towards the air intakes the flow separation along with the body of aircraft from nose till the air intakes is requires to be optimized or the air intakes are required to be designed in a shape to cater for this flow separation and maximize the pressure recovery at the engine compressor. As shown in figure 1 the pressure recovery is reduced because of this boundary

layer buildup which subsequently has a negative effect upon engine thrust.
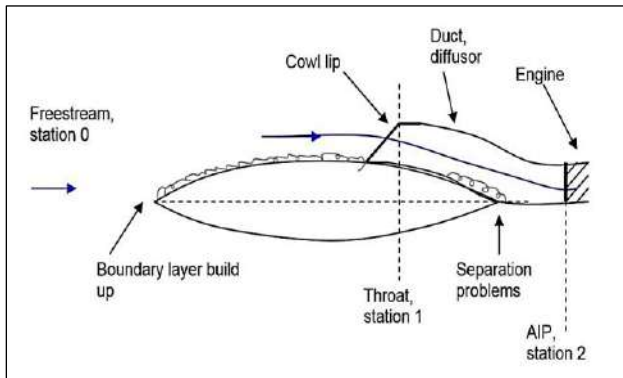
Figure 1: Typical Fighter Aircraft Intake showing flow separation problems

II. AIR INTAKES & FLOW OPTIMIZATION

Flow optimization at the region from nose till the air intakes is possible but has various limitations. Few practically viable techniques to reduce the boundary layer separation or unwanted build up include active & passive control methods. Optimum Trapped Vortex Cavity is one of the profoundly efficient and reliable methods to control the airflow which was notably improved in a recent study by [2] realizing a 31.8 % power-coefficient gain for vertical axis wind turbines with an optimized trapped-vortex cavity - the highest improvement reported for vertical axis wind turbines - while reducing CFD cost by 97 %. Power performance of 2-D H-type VAWT was increased by using an optimum cavity on NACA 0018 blade airfoil. Computational cost was reduced using the GPR (Gaussian Process Regression) model coupled with the Genetic Algorithm at static stall angle of attack in an isolated environment. 80 CFD simulations were run to reduce computational efficiency by 97% and it was confirmed in the results that aerodynamic efficiency of optimum cavity has only 0.5% difference with the predictions of GPR. In near stall regions 31.8% aerodynamic efficiency was improved due to utilization of optimum cavity on the VAWT airfoil in comparison to the clean surface. It depicts that such passive flow control methods being very cost effective and practically viable can also be used on air intakes to augment the performance and reduce pressure losses leading to enhanced intake performance for aircraft engine design. However, since in the air intakes the mass flow rate entering the engines is a critical control variable to determine the final thrust produced from propulsion viewpoint. The advantages gained in terms of reduced pressure losses & drag will have to be optimized for the demerits like increased complexity, careful maintenance & possible negative effects on air to fuel mixture ratio at the combustion chamber. But utilization of this concept for air intakes is still novel and careful CFD analysis can be carried out to cater for the flow optimization at the intakes using this method. However, alternatively in this paper flow optimization using DSI will be focused.

Since Artificial Intelligence has also taken over as a very fruitful tool to further enable the modern world technologies. Its employment in the problem of flow optimization can be considered as a very practical option as well. In conjunction with the conventional CFD methods AI based machine learning (ML) algorithms can be used to improve the design and functionality of wind turbine blades. In a recent study [3], AI based algorithms were used efficiently to optimize the geometry shapes of wind turbine blades to achieve the flow optimization & aerodynamic drag and turbulence were minimized without compromising the energy output. The study demonstrated how machine-learning (ML) frameworks, when coupled with high-fidelity CFD can compress design-cycle cost by orders of magnitude while delivering record-level aerodynamic gains. These advances open a clear pathway for ML-guided tailoring of diffuser and inlet-duct profiles in high-performance aircraft, where precise control of inlet-distortion and pressure-recovery metrics is mission-critical. Therefore, ML algorithms can be explored as an effective tool to optimize the best suitable geometry profiles for the air intakes of fighter jets which will reduce the cost & effort and enhance the accuracy with which flow optimization problem can be addressed for the air intakes. However, since ML requires a baseline data set to process the optimization which might be a limitation for analysis of modification of air intakes of already operational fighter aircraft.

A complementary, and now widely adopted, passive-flow-control strategy is the bio-inspired leading-edge-tubercle geometry systematized in a recent study by [4]; notably, the scalloped profile that underpins this work also forms the conceptual basis of modern diverterless-supersonic-inlet (DSI) designs. Low power coefficient of VAWTs is a limitation which was enhanced by employment of tubercles by using hybrid design of Experiments (DoE) approach & Response Surface Methodology (RSM) instead of random values of tubercle variables & CFD was run on unsteady conditions using a four-equation transition SST turbulence model. At off design conditions maximum of 55 % performance was enhanced for the VAWT. Similar model / geometry profiling of air intakes may also be a possible way out to increase the pressure recovery which is still a novel concept when it comes to the air intake configurations keeping in view the existing types of air intakes [5] which are as following:-

- Submerged Air Intakes. The intakes is submerged into the main body of aircraft in order to reduce the drag and optimize the flow.
- Pitot Tube Intakes. It is just like a tube with aerodynamic faring around its lips. This intake design has divergent duct shaped interior to receive ram air at the entry and convert to ram pressure as maximum as possible before delivery to the compressor
- Bellmouth Intake. This is a funnel shaped entrance duct facilitating minimizing loss of entry. This design is used for an engine subject to ground test at the test cell. These types of intakes were introduced to lower the Vena Contracta Effect. This is the phenomenon of necking down of flow at the edges. Bellmouth inlets eliminate the contraction and allow air all the air it can handle
- Supersonic Intakes These are specifically designed for supersonic regimes and includes:-

- Normal shock wave intakes
- Oblique shock wave intakes
- Cone Intakes
- Ramp Air Intakes
- Diverter Less Supersonic Intakes (DSIs)

III. RAMP INTAKES & DSIS - A COMPARISON

An intake ramp is a rectangular, plate-like device within the air intake of a jet engine, designed to generate a shock wave to aid the inlet compression process at supersonic speeds. The ramp sits at an acute angle to deflect the intake air from the longitudinal direction. At supersonic flight speeds, the deflection of the air stream creates an oblique shock wave at the forward end of the ramp. Air crossing the shock wave suddenly slows to a lower Mach number, thus increasing pressure. [6]

Ideally, the oblique shock wave should intercept the air intake lip, thus avoiding air spillage and pre-entry drag on the outer boundary of the deflected stream tube. For a fixed geometry intake at zero incidence, this condition can only be achieved at one particular flight Mach number, because the angle of the shock wave (to the longitudinal direction) becomes more acute with increasing aircraft speed. Some supersonic intakes feature two or more ramps, operating in series, to generate multiple oblique shock waves. Each downstream ramp is steeper in inclination than the previous ramp. These intakes are usually more efficient than single (oblique) shock wave inlets.

Whereas, a Diverter less Supersonic Intake (DSI) is a type of jet engine air intake used by some modern combat aircraft to control air flow into their engines. It consists of a "bump" and a forward-swept inlet cowl, which work together to divert boundary layer airflow away from the aircraft's engine. This eliminates the need for a splitter plate, while compressing the air to slow it down from supersonic to subsonic speeds. The DSI can be used to replace conventional methods of controlling supersonic and boundary-layer airflow [7].

It was compared with a traditional "caret" style inlet. The trade studies involved additional CFD, testing, and weight and cost analyses. The new inlet earned its way into the JSF design after proving to be thirty percent lighter and showing lower production and maintenance costs over traditional inlets while still meeting all performance requirements. [8].

Accurate CFD–experiment correlation is indispensable for refining diverterless-supersonic-inlet (DSI) bump geometries, yet the compound curvature of a DSI makes conventional machined or wooden wind-tunnel models both labor-intensive and dimensionally unreliable. However, this long-standing bottleneck was removed in the recent study by [9] introducing a high -fidelity, improved additive-manufacturing workflow that yields models with high precision and reduces fabrication lead-time significantly; thereby establishing a robust benchmark for closing the CFD–experiment loop and enabling rapid, low-cost validation of optimized DSI bump profiles.

Accelerated air flow performance is crucial role of high lift devices and an air intake is essentially supposed to accelerate the airflow. However, the design of DSIs is an iterative process which requires extensive analysis in CFDs or wind tunnels but these methods have very high computational costs and are time consuming. A robust framework based on Potential Flow Solver (PFS) & geometry parameterization has been developed [10] & [11] without compromising the fidelity of the analysis using the Vortex Lattice Method (VLM) coupled with Polhamus Suction Analogy and parametric modeling of high lift devices and computational cost of CFD was reduced to three times; enabling exploring the optimized bump configurations for the aircraft in less time yet with high fidelity.

CFD is essential for optimization of airflows across air intakes or other aerodynamic applications, however, turbulence modelling is very expensive in high fidelity CFD and it requires a lot of time. AI based turbulence modelling framework has been introduced in a recent study [12] which has proposed integration of Physics-Informed Neural Networks (PINNs) with traditional CFD solvers to accelerate high-fidelity simulations. As per results AI-augmented CFD simulations were found to be 70% faster due to which cost and time has been reduced significantly and accuracy has been preserved at the mean time. Moreover, AI based model has captured the complex flow structures & interactions effectively.

Furthermore, efficiency & performance of air intakes is critically linked to the bump because the shape optimization of aerodynamic surfaces plays a key role in deciding the performance. In routine optimization methods expensive CFDs are carried out however in advanced AI based techniques which have been presented in recent study [13], a Generative AI-driven aerodynamic shape optimization framework has been proposed which leverages deep neural networks to streamline the optimization process. Generative adversarial networks (GANs) and variational auto encoders (VAEs) were used to generate and refine aerodynamic shapes with optimal performance metrics. Physics informed ML was incorporated and benchmark case studies including airfoil and automotive body designs were optimized using this AI driven shape optimization model. Superior efficiency was recorded in comparative analysis again adjoint-based solvers.

In addition, Adjoint-based optimization is an effective tool for increasing the aerodynamic performance. A recent study [14] conducted adjoint-based shape optimization of the RAE-2822 airfoil at transonic Mach numbers and benchmarked two parameterization strategies—Hicks-Henne bump functions and Free-Form Deformation (FFD)—within a fully coupled discrete-adjoint framework. The framework yielded a 67 % reduction in total drag and a three-fold gain in aerodynamic efficiency, while simultaneously generating a quantitative metric set for cross-comparing parameterization methods. Because of the exceptional control authority, it delivers with a markedly smaller set of design variables (proven in the study), the Free-Form Deformation (FFD) can be adopted for parameterizing next-generation fighter-jet intake bumps, allowing researchers to probe a substantially broader design envelope while keeping the optimization process fully computationally tractable.

DSIs completely eliminates all moving parts. This results in an inlet that is far less complex than earlier diverter-plate inlets. The removal of moving parts also lightens the overall weight of the aircraft. Traditional aircraft inlets contain many moving parts and are much heavier than newer Diverter Less Intakes.

DSIs also crucially improve the aircraft's very-low-observable characteristics (by eliminating radar reflections between the diverter and the aircraft's skin). Additionally, the "bump" surface reduces the engine's exposure to radar, significantly reducing a strong source of radar reflection because they provide an additional shielding of engine fans against radar waves.

A framework was proposed in recent study [15] for accurate quantification of a die-casted wing using laser scanning and reverse engineering technique which present quick manufacturing solutions with great precision. Coordinate Measuring Machine (CMM) was used to scan the upper and lower wing and data was exported to CAD software from where surface was generated using Free Form Reverse Engineering (FFRE). Deviation analysis for inaccuracies originating due to manufacturing and data acquisition was carried out. The wing was later analyzed by the point data to 3D CAD model for deviation. It minimized the data acquisition and data processing error and allowed deviation to be solely traced back to the manufacturing technique. Similar technique can be used for fabrication of divertlerless air intakes to reduce the manufacturing errors.

IV. PREPARATION OF DSI GEOMETRIES & CAD MODELLING

To understand the flow behavior over the bump, four different designs of bumps were created in MATLAB®. The above formula was implemented in MATLAB® and 3D surface was generated. All bumps have same dimensions but their shapes are different to investigate the difference of the flow over a variety of shapes. Details are as under:-

Table 1: Bump Dimensions

	Smaller	**Softer**	**Blunter**	**Original**
Length	1.4	1.4	1.4	1.4
Width	0.775	0.775	0.775	0.775
Height	0.10	0.20	0.20	0.22
Max Amplitude	0.88	0.83	0.79	0.84

The curve geometries created in MATLAB® are shown in the Figures 2, 3, 4 & 5. Whereas, Figure 6, 7 & 8 shows the CAD Model in CATIA.
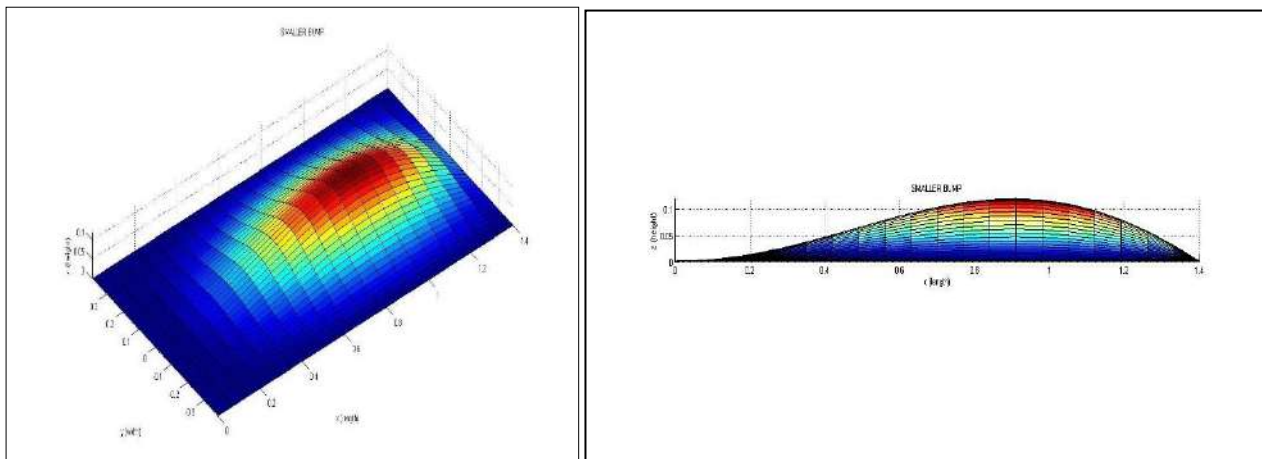
Figure 2: Smaller Bump (Top & Side View)
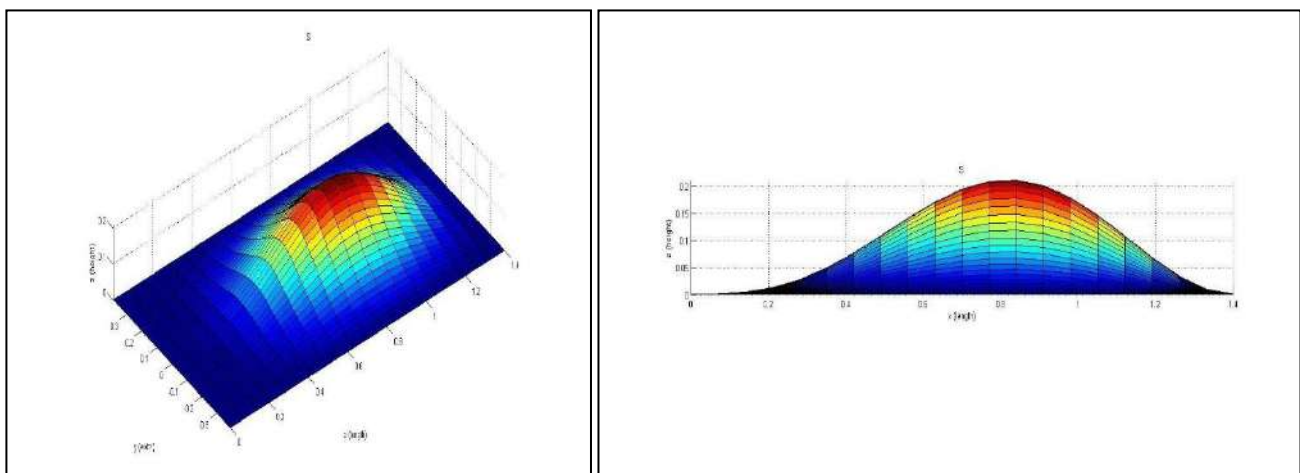

Figure 1: Softer Bump (Top & Side View)
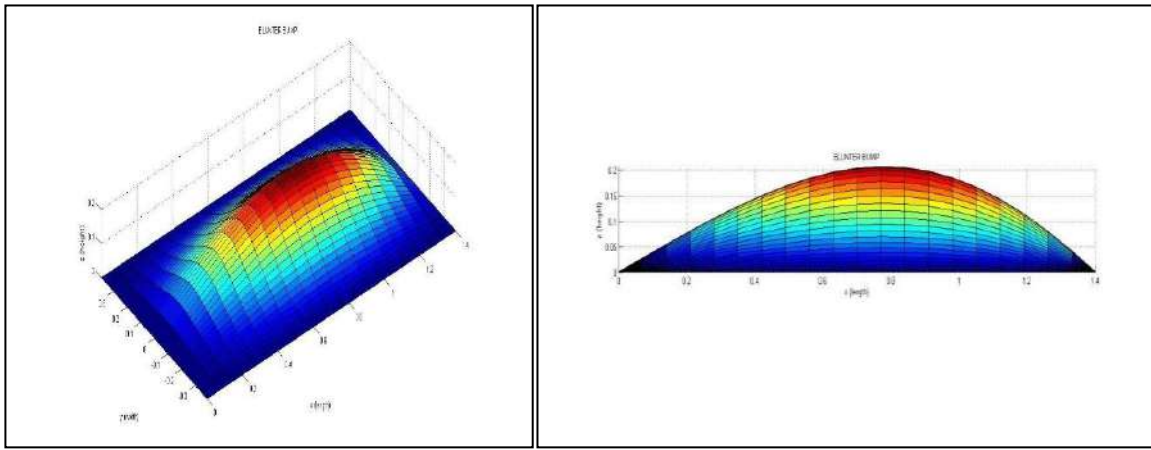
Figure 2: Blunter Bump (Top & Side view)
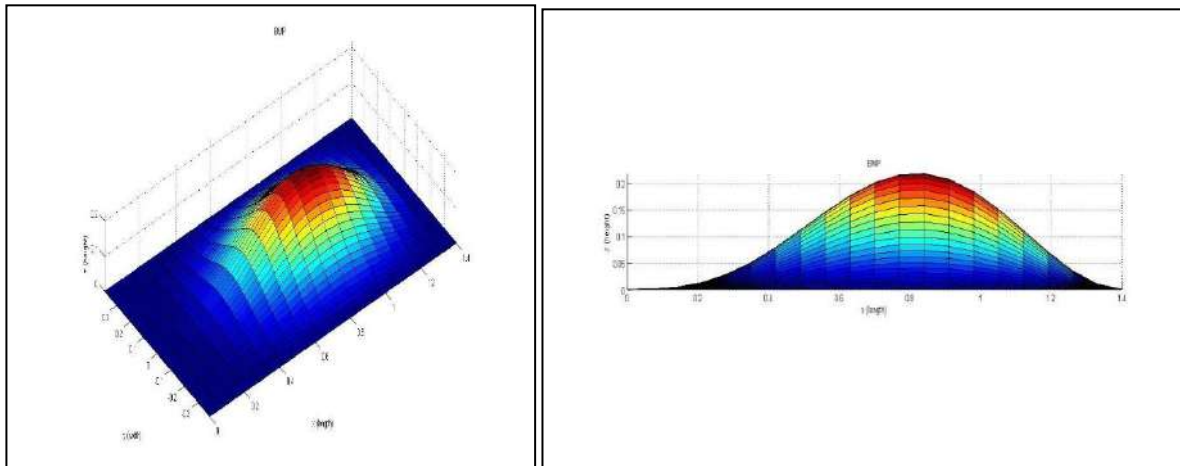
Figure 3: Original Bump (Top & Side View)

MATLAB surfaces can only be saved in limited formats like JPEG, PNG or FIG [16]. These geometries could not be saved in some CAD format. So, points from MATLAB® were extracted to excel sheet & subsequently associated with CATIA and then simply by just drawing splines geometry is modelled followed by "multi-section solid" command was used to draw final geometries. So, advantage of coding in MATLAB is that to alter various profiles of geometry in CATIA only small change in the code is required and complete 3D CAD model is altered accordingly [17]. Final CAD models thus obtained are as under:-
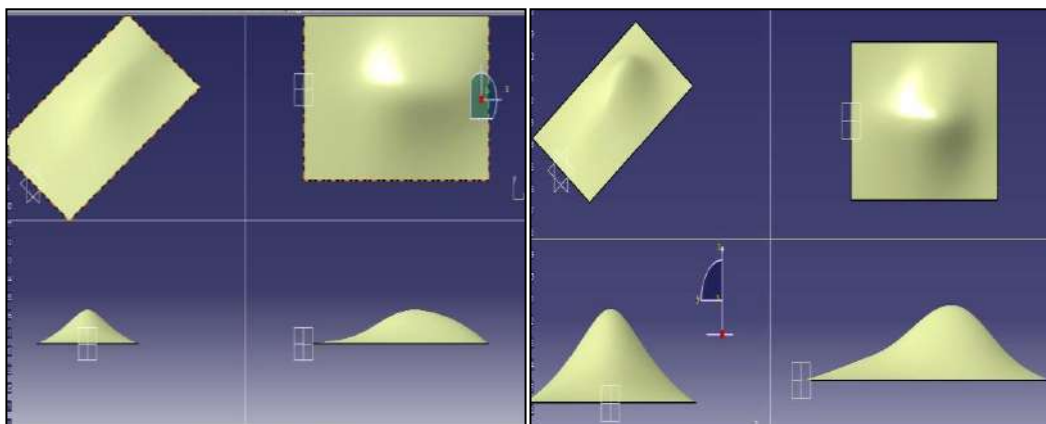
Figure 4: Smaller Bump (Left), Original Bump (Right)
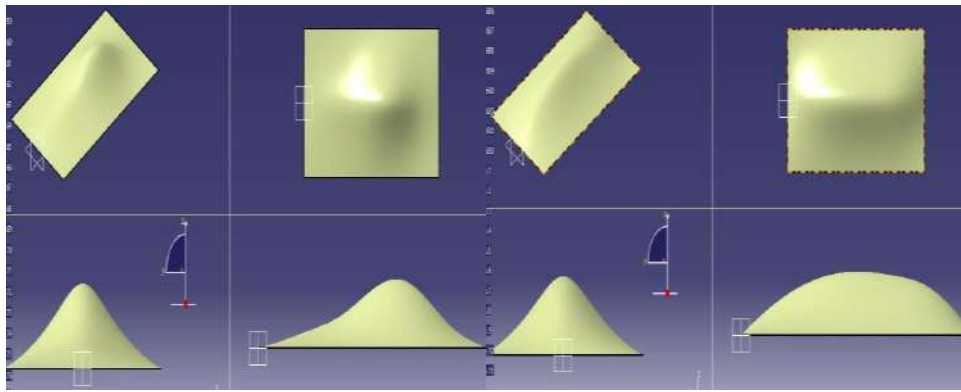
Figure 5: Softer Bump (Left), Blunter Bump (Right)
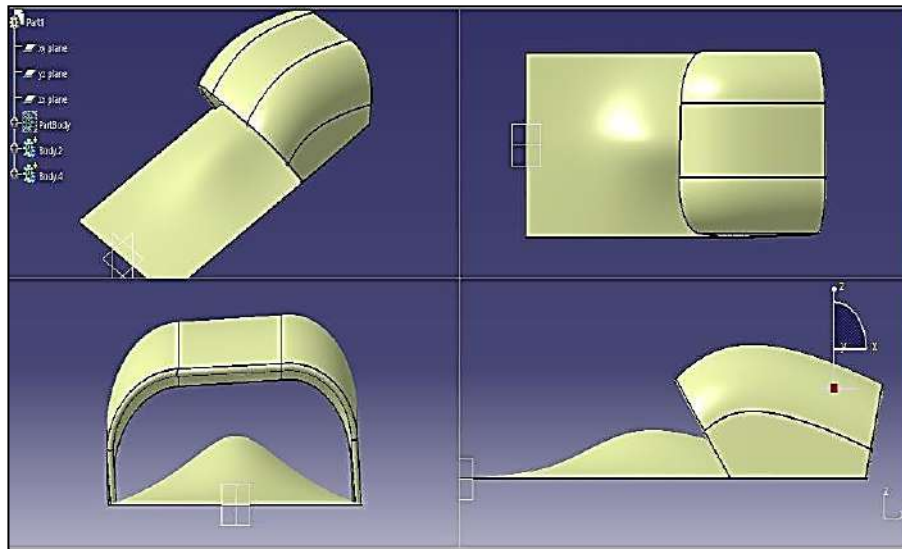
Figure 6: Diverter less Air Intakes

V. SETUP OF COMPUTATIONAL FLUID DYNAMICS (CFD)

CFD was used to analyze the flow characteristics (turbulence) over the bumps in DSIs CAD models. Turbulence modeling can be done either using Reynolds-Averaged Navier-Stokes equation (RANS) or for more accuracy by Reynolds stress models or LES are used [18]. Subsequently, discrete solution at the grids for the flow variables p V r, etc. is obtained by CFD for the governing partial derivative equations. Repetitive calculations are carried out for the matrix inversion problem. Setting up the discrete system and solving it (which is a matrix inversion problem) involves a very large number of repetitive calculations and is done by the digital computer. Triangular mesh technique was used for the generation of surface mesh. The elements size was given individually to each element. Areas of major concern were given finer mesh size. Then mesh was computed on all geometries by keeping in mind the computational resources and level of accuracy [19]. Five no of layers were used on prism layer to capture the boundary layer effects. Tetra size ratio was defined to be 1.2. All tri mesh type was selected to create triangular elements over the whole surface. Mesh type selected was the Patch Independent. The patch independent mesh does not follow the curves in the geometry strictly hence gives a more uniform mesh [20]. The total number of elements and quality of mesh for all the geometries are shown in the table 2 below.

Table 2: Mesh Qualities

Geometry	Total No of elements	Min Quality
Bump original with intake	3149100	0.33
Bump blunt with intake	3151346	0.30
Bump smaller with intake	3153648	0.30
Bump softer with intake	3158373	0.29
Bump original	282111	0.40
Bump blunt	2834166	0.39
Bump smaller	2802300	0.41
Bump softer	2813207	0.38

No single turbulence model is universally accepted as being superior for all classes of problems [21]. The choice

of the turbulence model depends upon the level of accuracy and available computational resource. The availability of time also marks its significance in the importance of turbulence model selection. The one-equation Spalart-Allmaras (SA) turbulence model was used due to its demonstrated feasibility for Aerospace applications, such as the present configuration. Although Spalart-Allmaras is a low Reynolds number model, however for the wall treatment, standard wall functions formulation of Fluent for SA model was used. Ideal Air was selected as the inlet fluid for the simulations. Explicit formulation method was selected.

The boundary conditions used for this analysis are shown below in the Table 3.

Table 3: Boundary Conditions

Domain	Boundary conditions
Farfield	Pressure Farfield
Near bump	Wall
Bump	Wall
Bottom	Wall
intake	Wall

VI. RESULTS OF CFD SIMULATIONS

Streamline contours were obtained at Mach 0.6 (sub-sonic) regime for each bump and the streamline contours for Bump Original, Bump Blunt, Bump Soft & Bump Smaller are presented in Figure 9, 10, 11 & 12 respectively:-
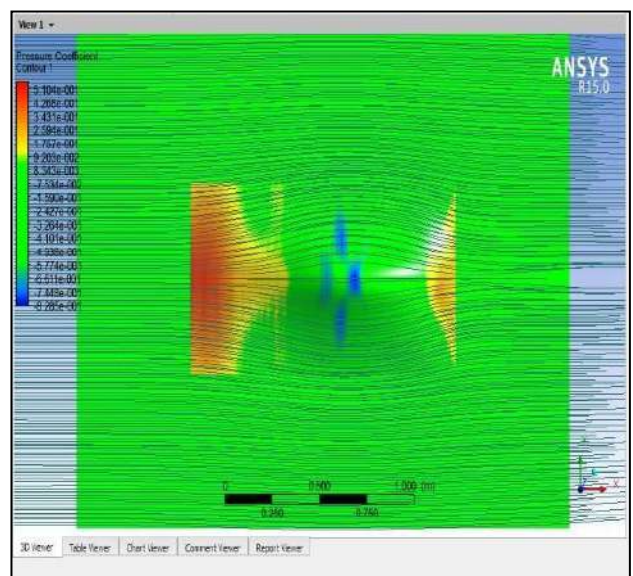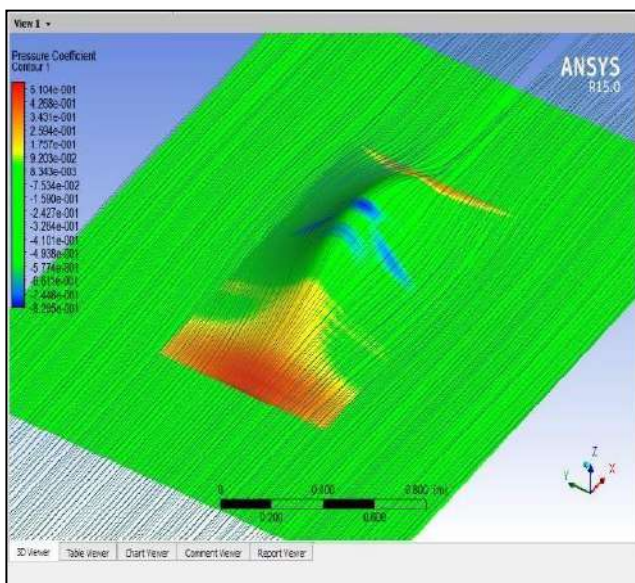

Figure 7: Bump Original at 0.6 Mach
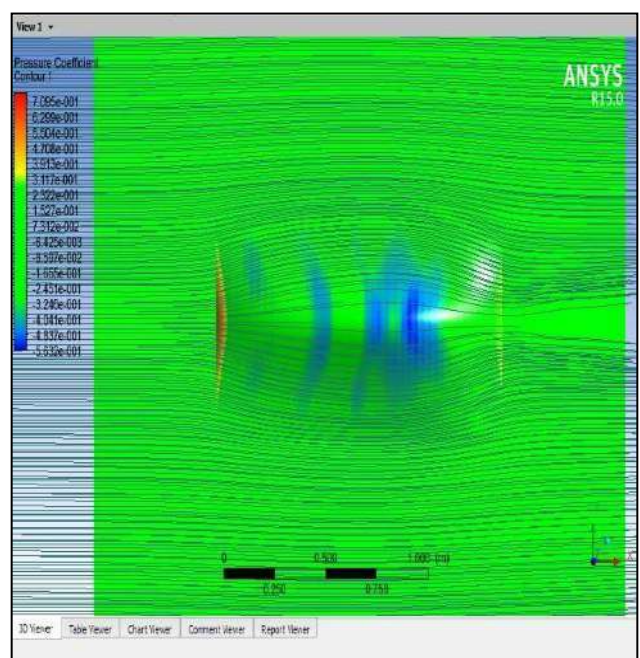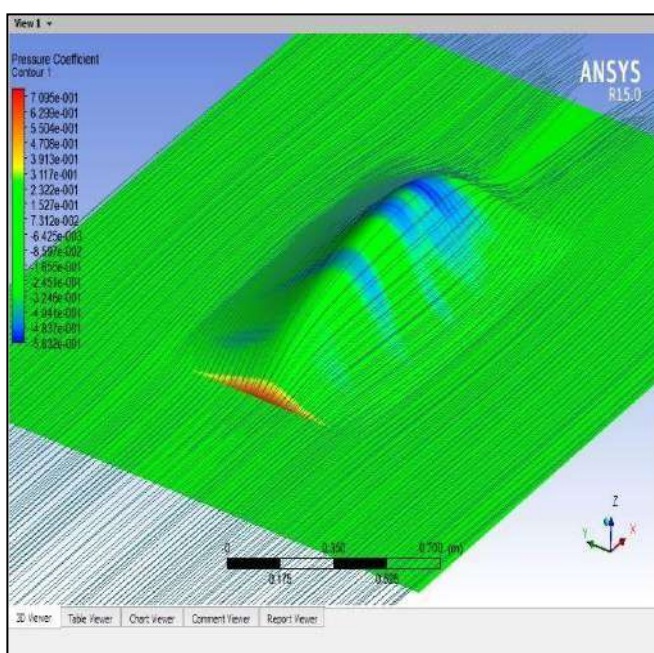
Figure 8: Bump, Blunt at Mach 0.6
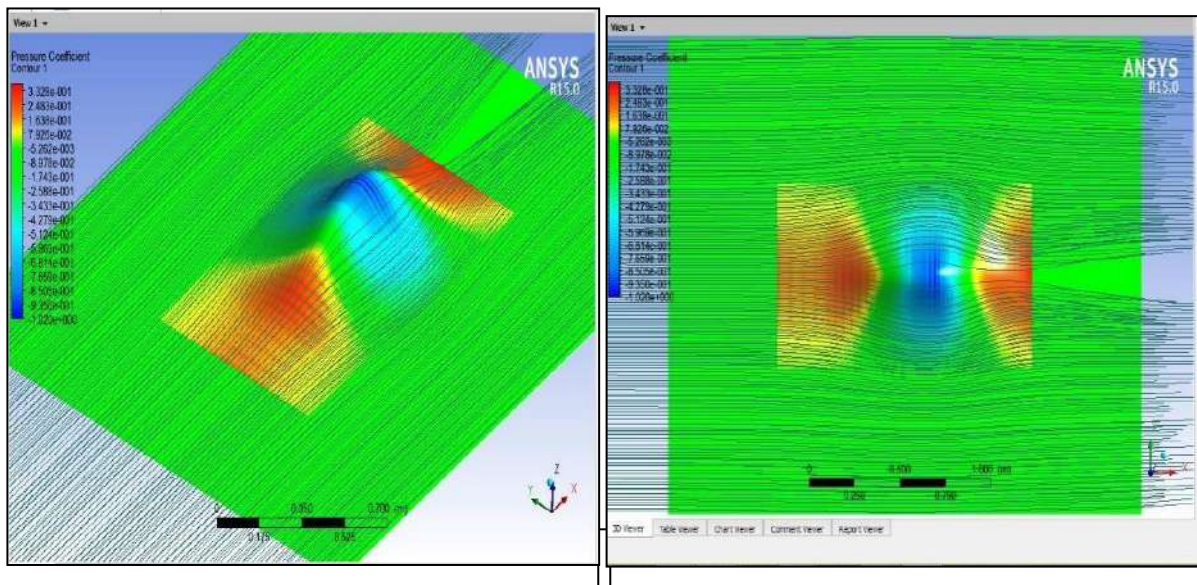
Figure 9: Bump Soft at Mach 0.6
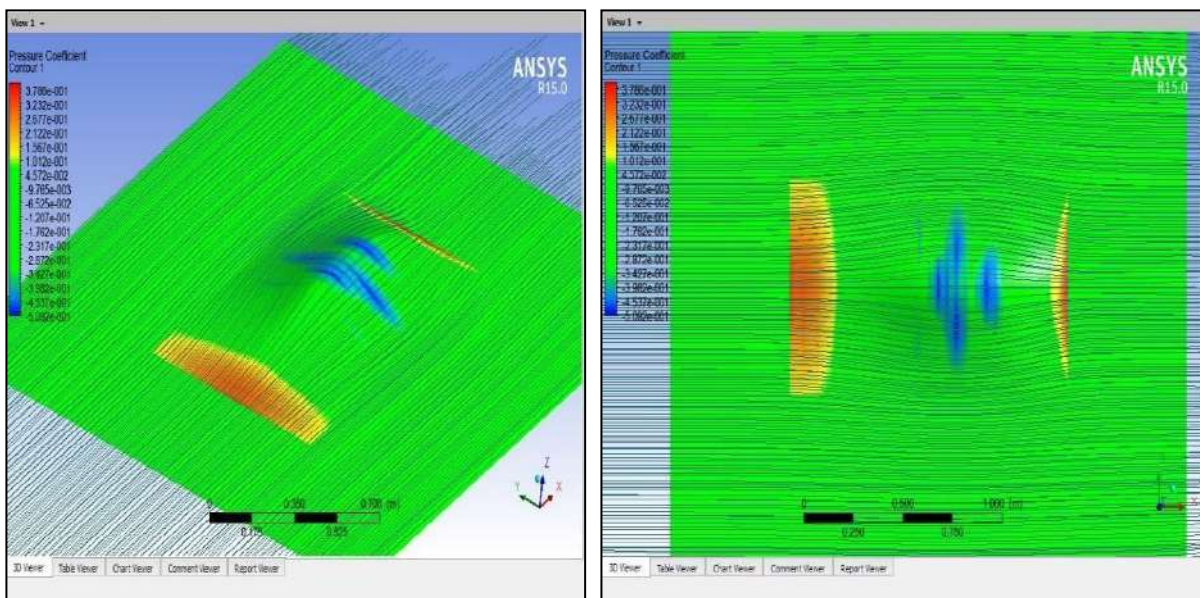
Figure 10: Bump Smaller at Mach 0.6

For supersonic regime streamline contours obtained are presented in Figure 13, 14, 15 & 16 for original, blunt, soft and smaller bump configurations.
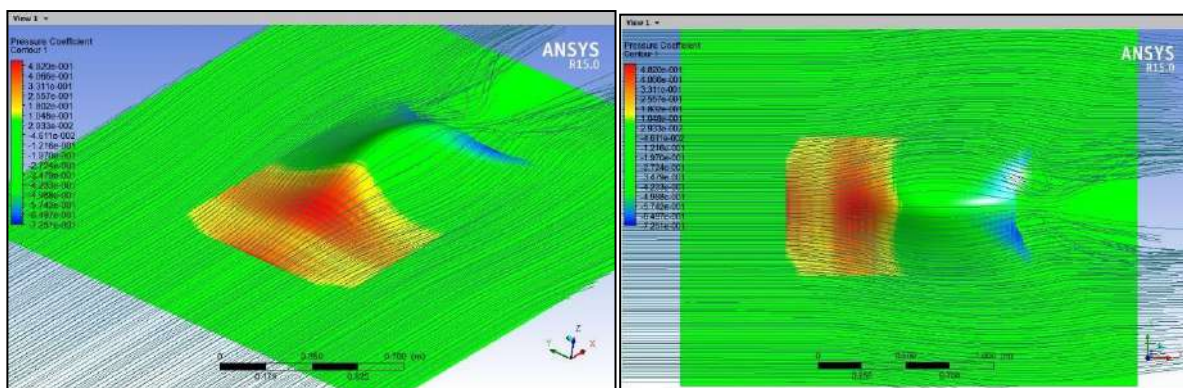

Figure 11: Bump Original Mach 1.2
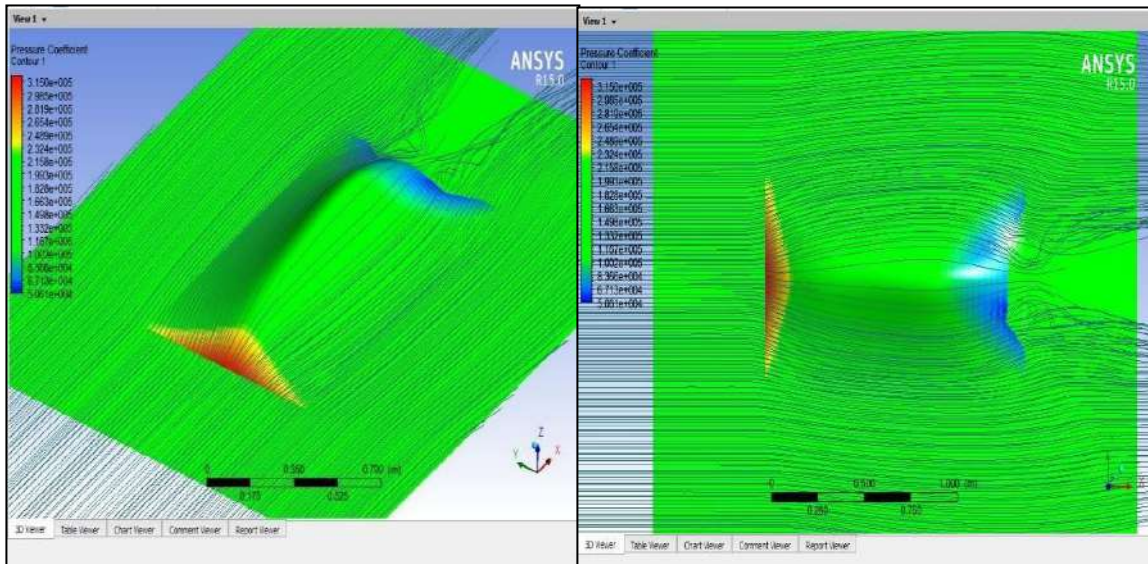
Figure 12: Bump Blunt at Mach 1.2
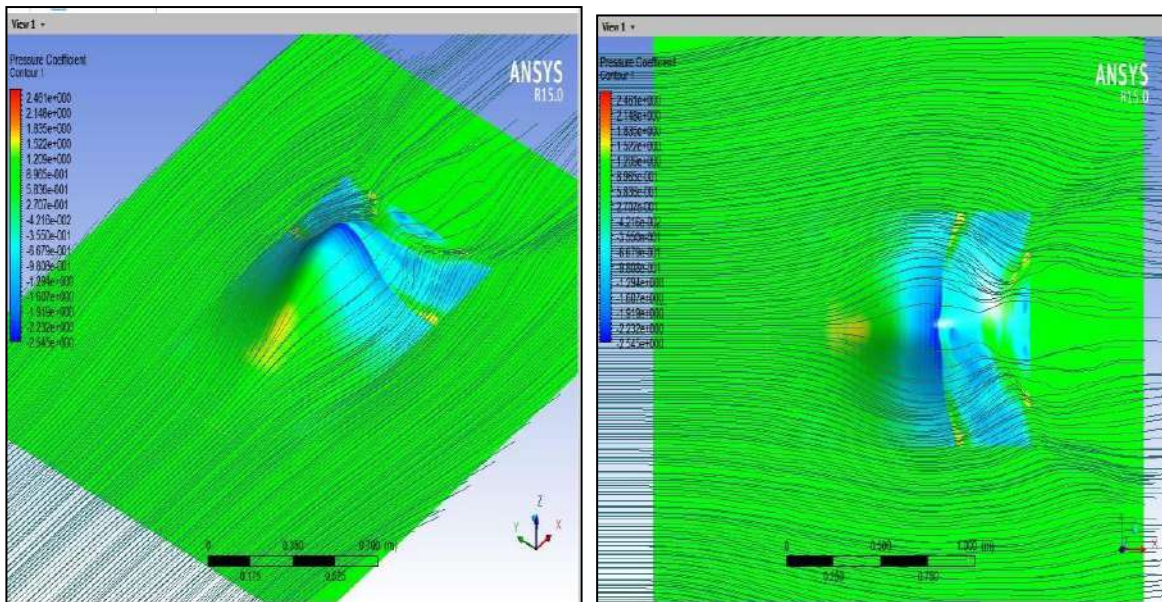

Figure 13: Bump Soft at Mach 1.2
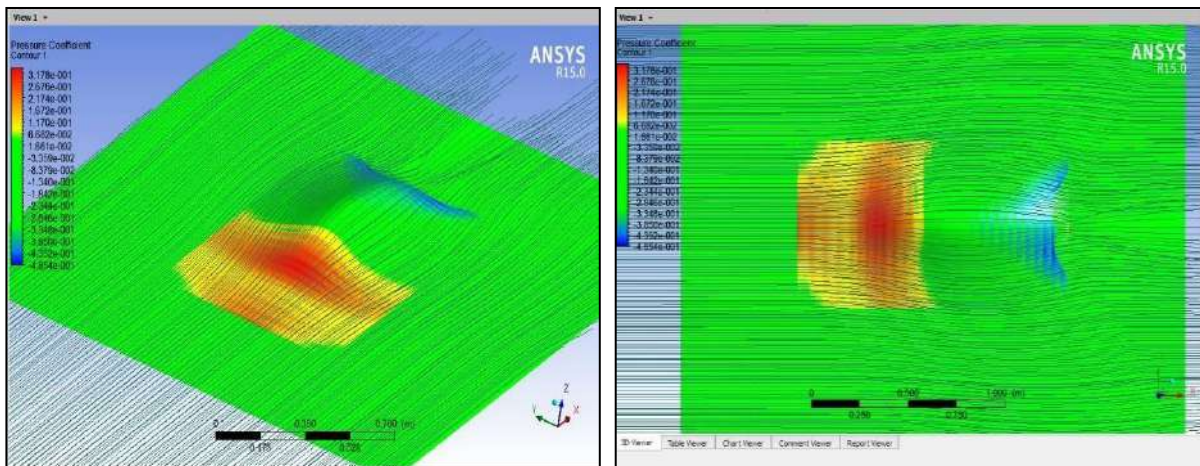
Figure 14: Bump Smaller at Mach 1.2

VII. MACH CONTOURS

The Mach contours can be seen for original, blunt, soft and smaller bump configurations in Figures 17, 18, 19 and 20 respectively.
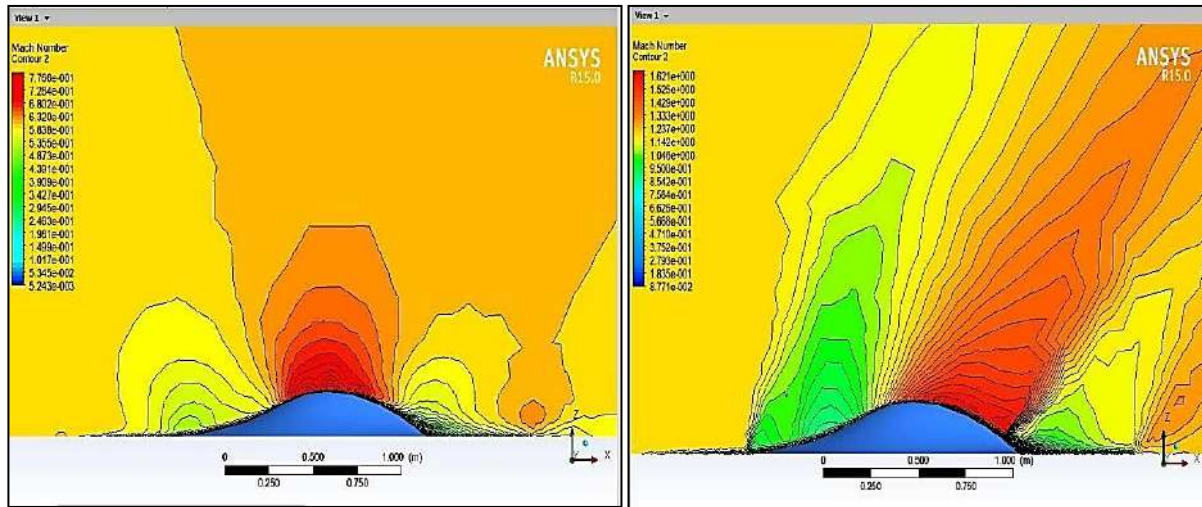

Figure 15: Original Bump at Mach 0.6 and 1.2
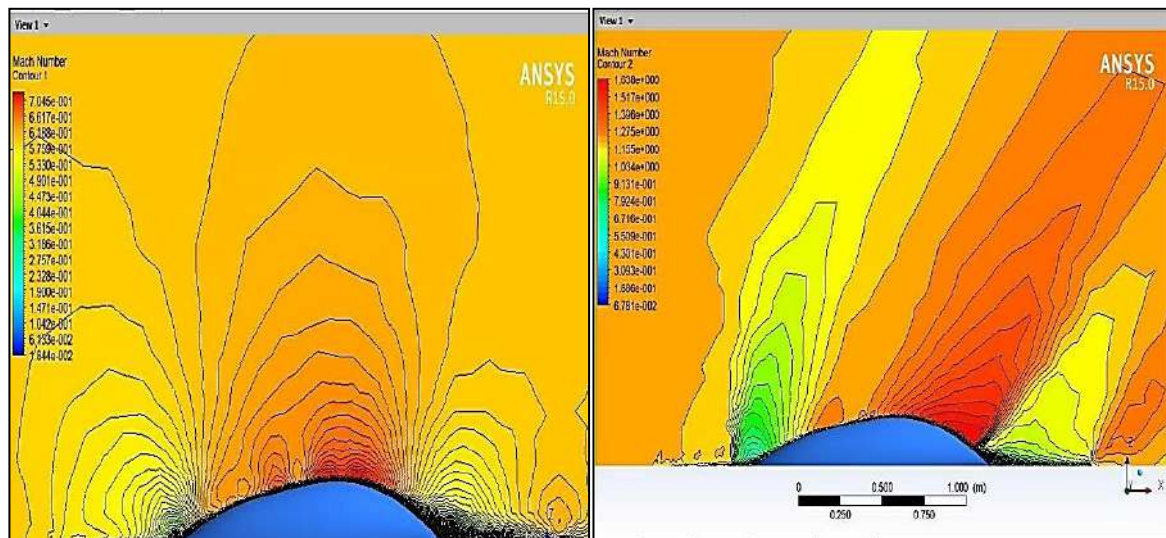

Figure 16: Blunt Bump at Mach 0.6 and 1.2
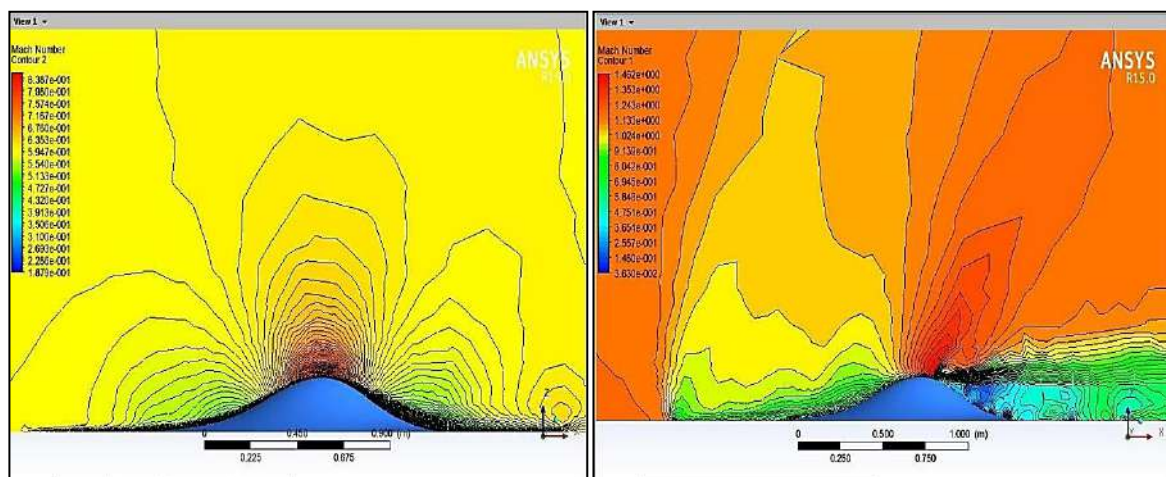
Figure 17: Softer Bump at Mach 0.6 and 1.2
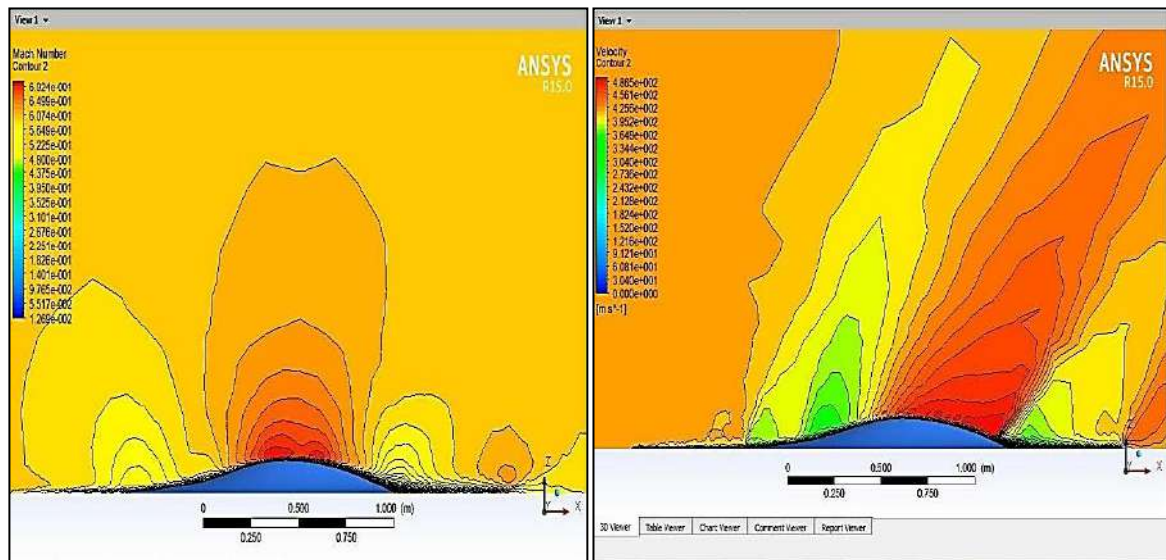
Figure 18: Bump Smaller at Mach 0.6 and 1.2

All these bumps were integrated with the air intake; shock wave forms and we can also visualize the flow qualitatively. For bump original, blunt, soft and smaller formation of shock waves is presented in figure 21, 22, 23 and 24 respectively.
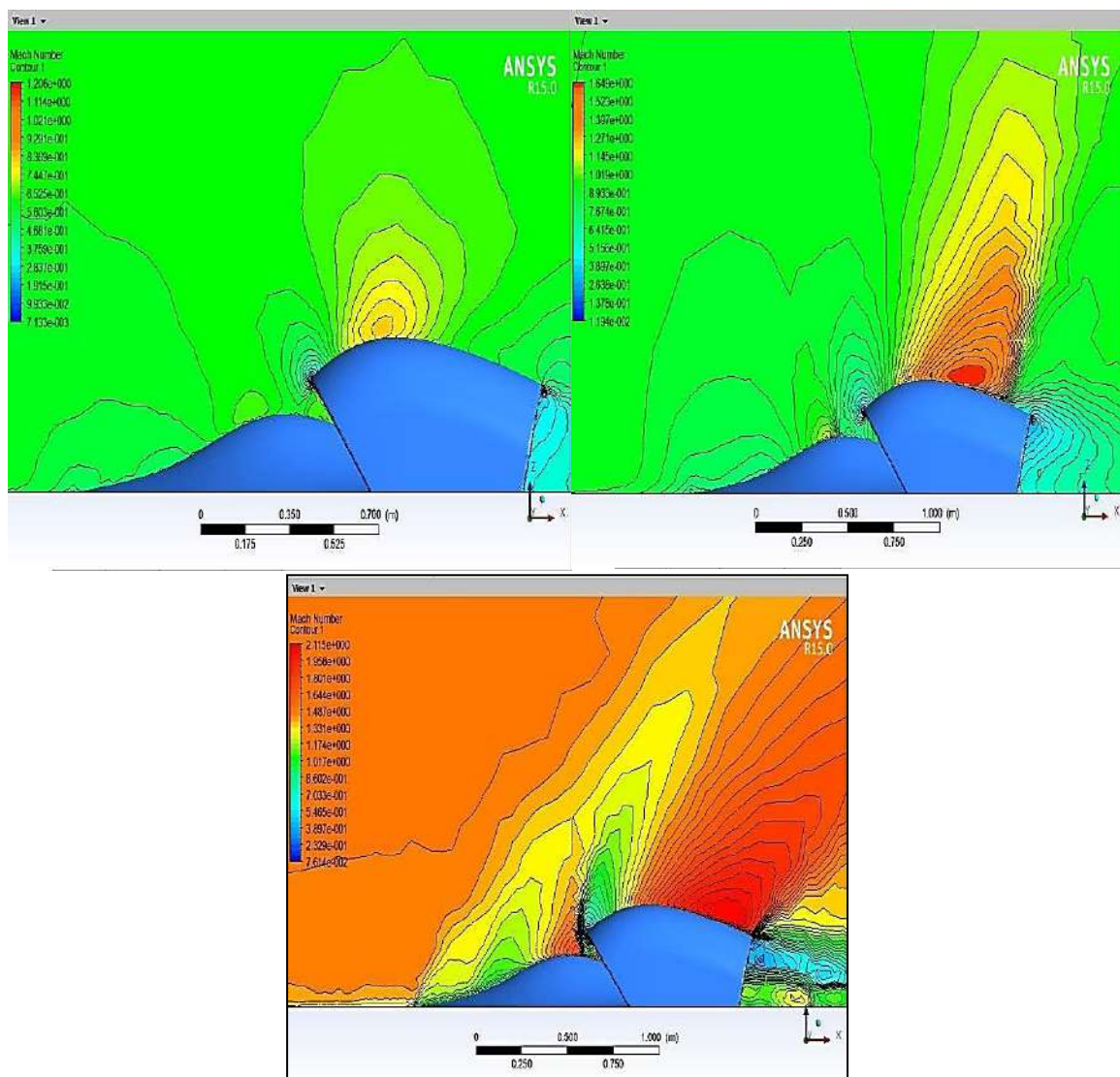

Figure 19: Mach contours original bump with intake at Mach 0.6 (Left), Mach 1.2 (Middle) & Mach 1.5 (Right)
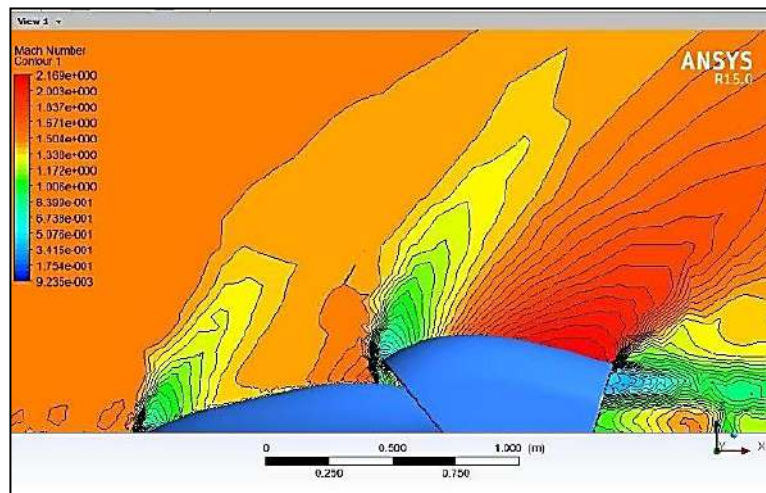
Figure 20: Mach contours soft bump with intake at Mach 0.6 (Left), Mach 1.2 (Middle) & Mach 1.5 (Right)
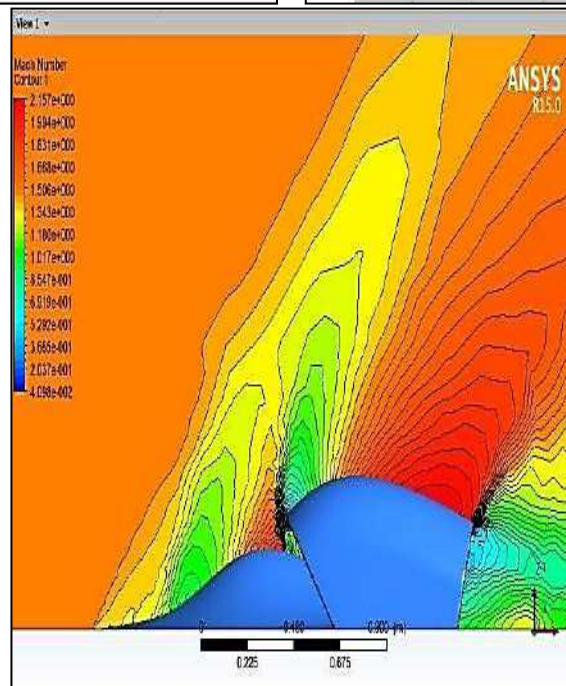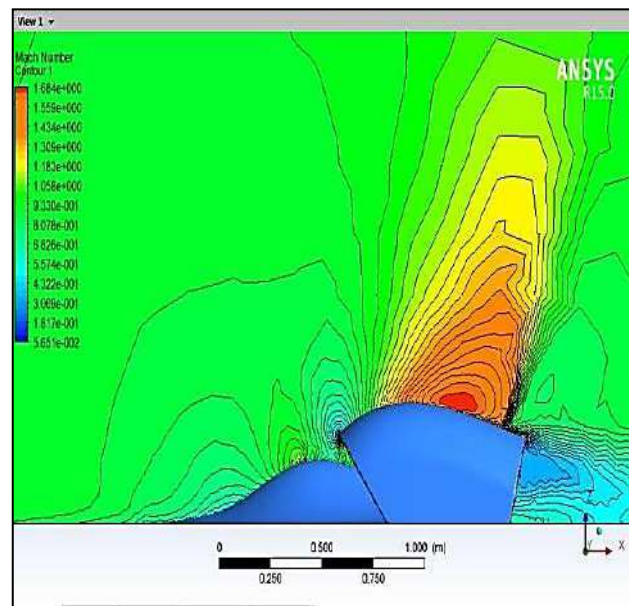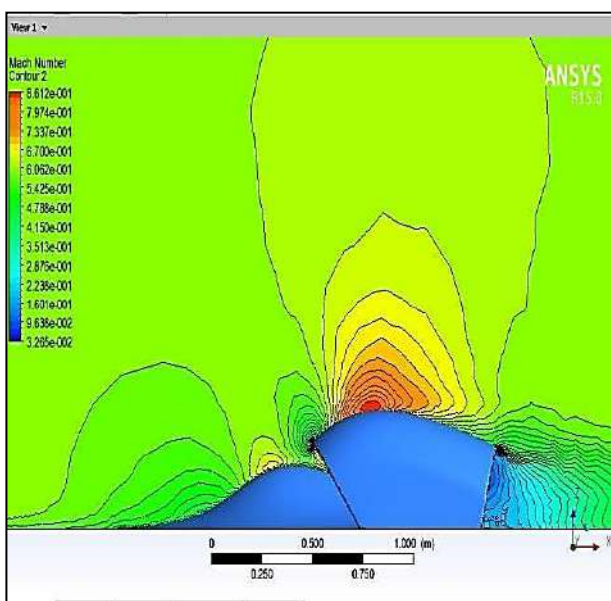
Figure 21: Mach contours blunt bump with intake at Mach 0.6 (Left), Mach 1.2 (Middle) & Mach 1.5 (Right)
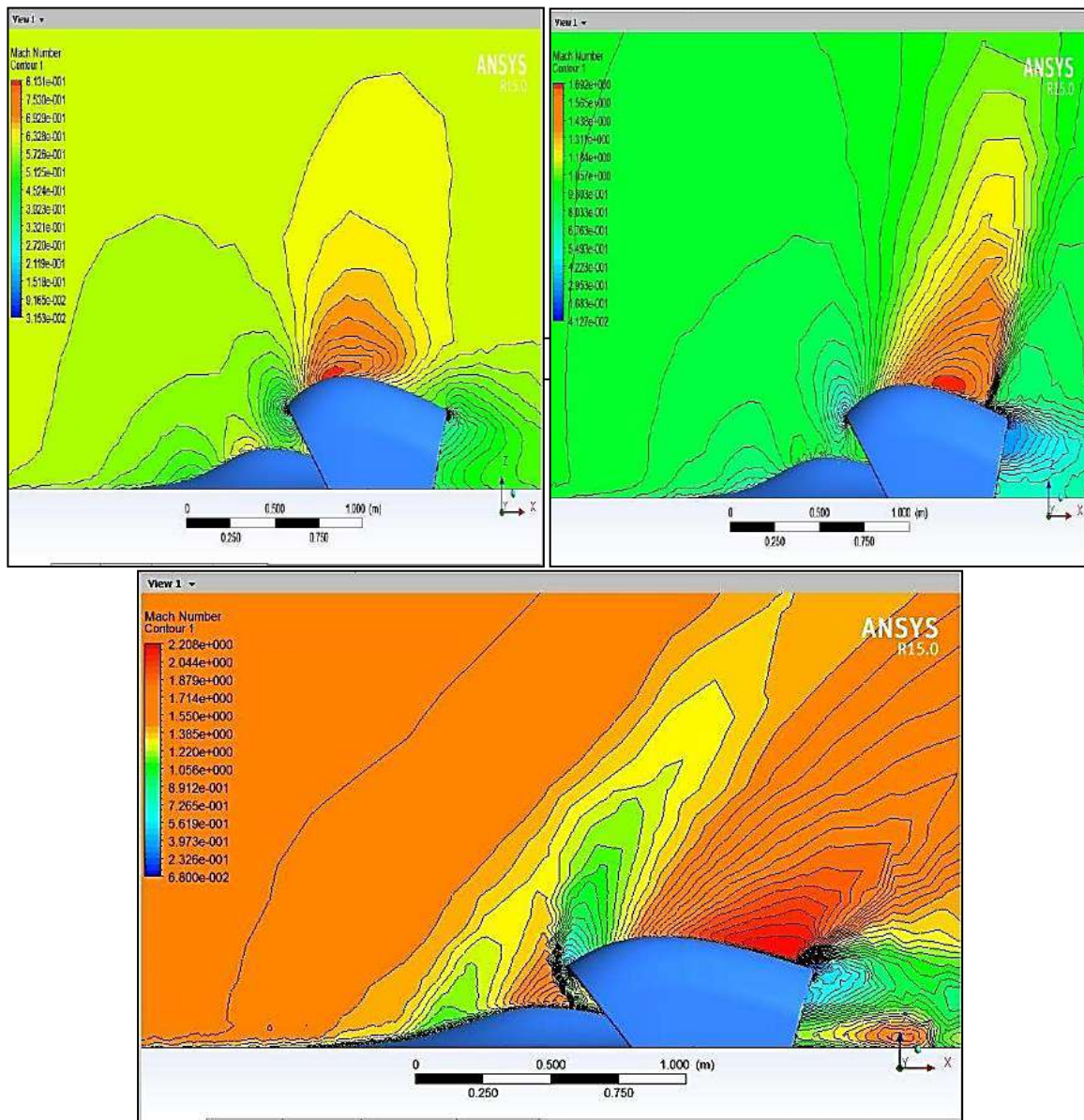
Figure 22: Mach contours smaller bump with intake at Mach 0.6 (Left), Mach 1.2 (Middle) & Mach 1.5 (Right)

VIII. PRESSURE CONTOURS

Pressure contours are also plotted for all these cases discussed above. The use of contour plots is usually not targeted for precision evaluation of the numerical values between contour lines. So, we can only visualize the flow and its behavior when it comes across different obstacles. Figure 25 represents pressure contours for original bump intake at Mach 0.6, 1.2 and 1.5.
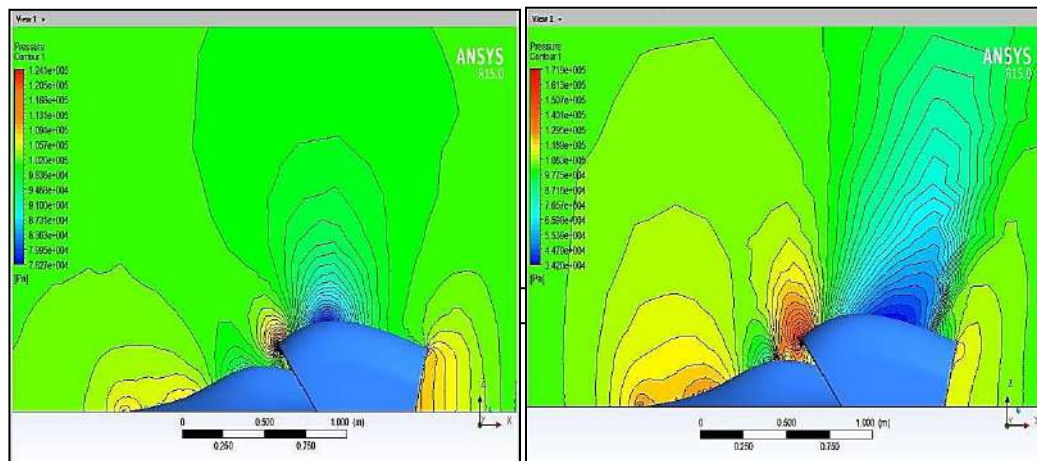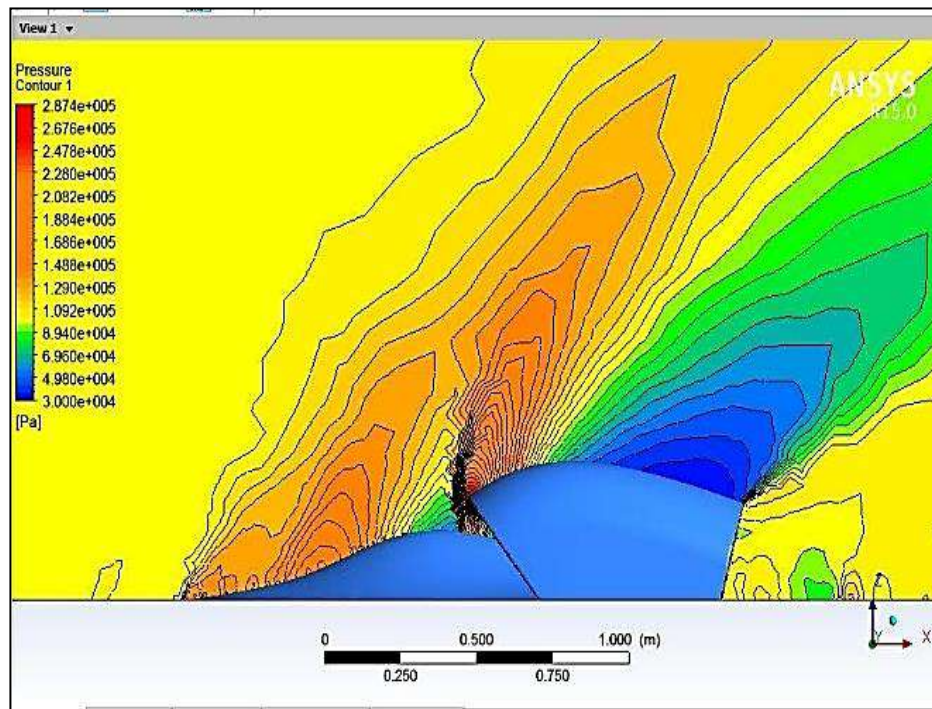
Figure 23: Pressure contours original bump with intake at Mach 0.6(Left), 1.29 (Middle) & 1.5(Right)

As we know pressure and velocity are inversely proportional to each other. So, these contours are exactly opposite to the Mach contours. As at the start of bump surface due to compression, the pressure increases so there we can see red areas representing high pressure locations. Across the shock wave the pressure is increasing.

Therefore, at the supersonic speed there forms a shock wave and it can be clearly seen in the figure 25. One shock wave is also forming at cowl lip of intake duct. For blunter bump formation of pressure contours at Mach 0.6 , 1.2 and 1.5 is presented in figure 26.
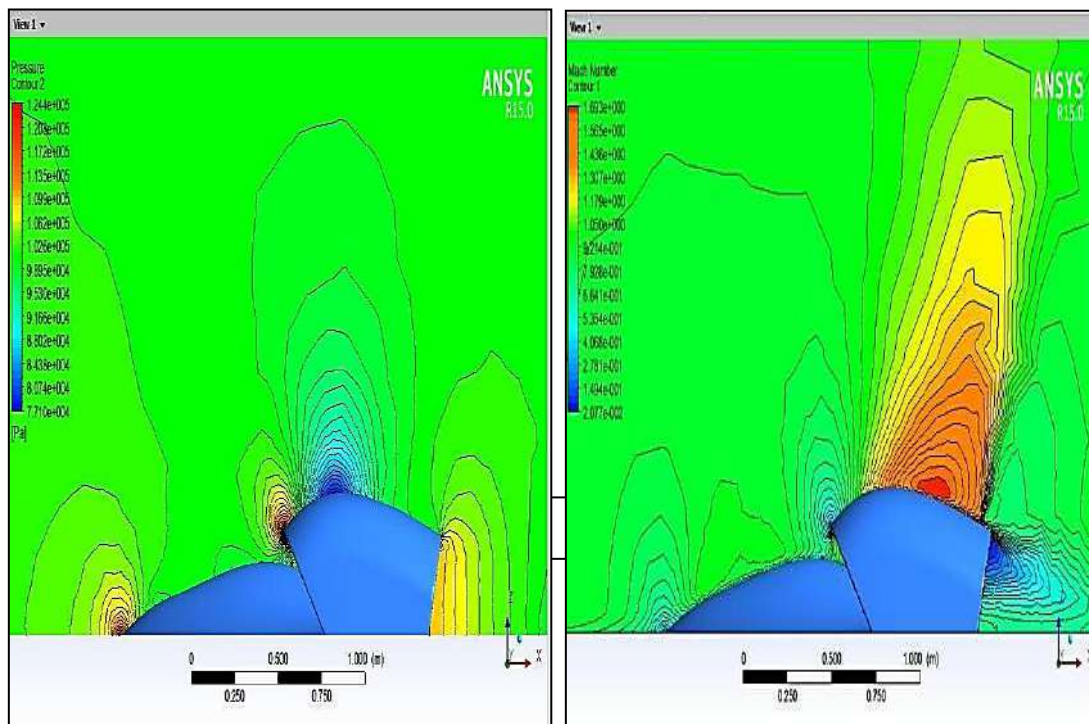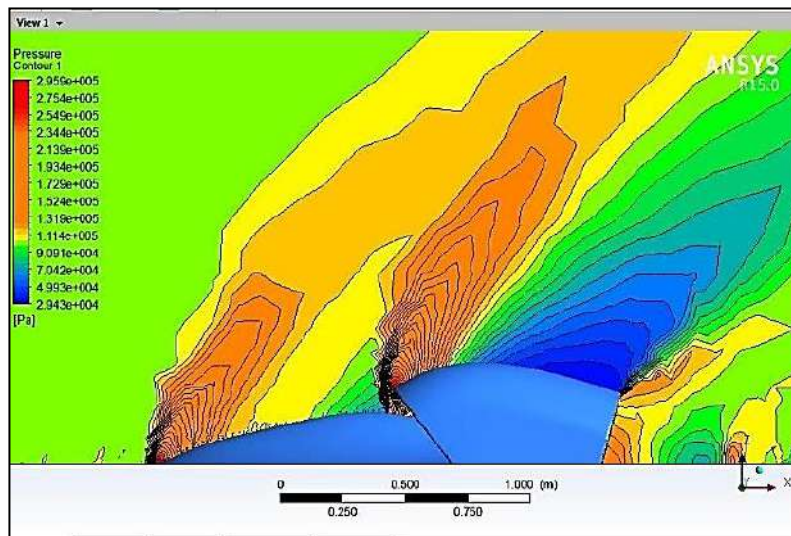
Figure 24: Pressure contours blunter bump with intake at Mach 0.6(Left), 1.29 (Middle) & 1.5(Right)

Many isentropic shocks waves form on these compression surfaces which combine to produce a strong shock wave.

Here these shock waves are eliminated in Figure 26 at much upstream of the intake duct.
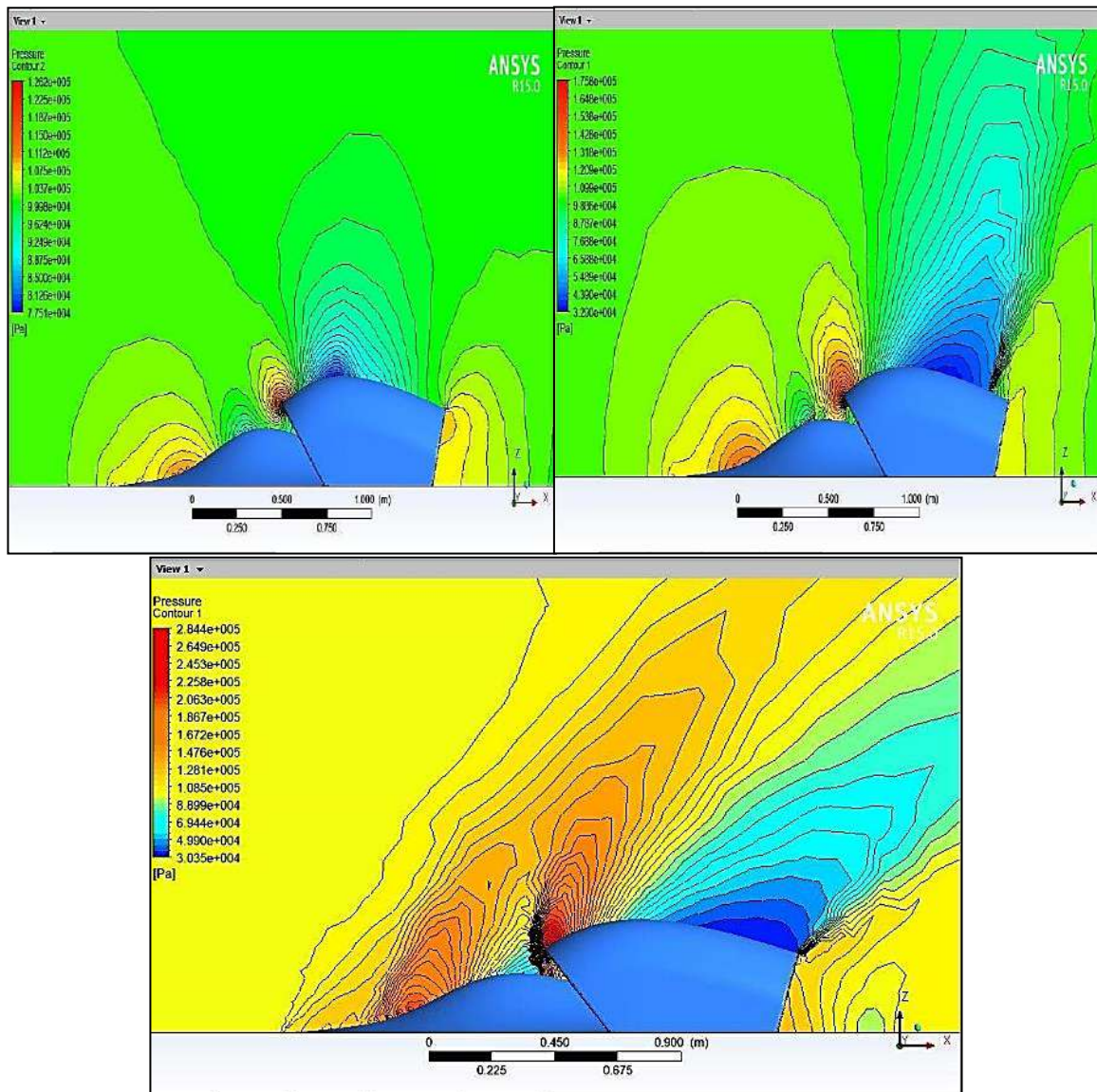
Figure 25: Pressure contours softer bump with intake at Mach 0.6(Left), 1.29 (Middle) & 1.5(Right)

IX. PRESSURE RECOVERY

The pressure recovery of all geometries can be seen below in the Table 4 given. A plane at the end of intake duct was made. This plane was of the same size as intake duct at the end. Then pressure recoveries were each other. These calculations are shown below:

We can see that there in not much difference in pressure recoveries at subsonic Mach. Bump smaller gives highest pressure recovery at 0.6 Mach. But there is not much difference in pressure recovery for all bumps at subsonic speed. When we reach transonic or supersonic Mach then this pressure recovery becomes more critical. Even very small gain in pressure recovery could make a lot of difference in efficiency of intake. So, we see here bump original maller are giving higher pressure recoveries as compared to other bumps.

Table 4: Pressure recovery comparison

Mach no.	Bump original	Bump Blunter	Bump softer	Bump smaller
0.6	0.945	0.946	0.941	0.952
0.95	0.856	0.840	0.836	0.868
1.5	0.779	0.738	0.748	0.754

X. ANALYSIS & DISCUSSION

Turbulence of flow can be indicated by the streamlines above the surface with the help of swirls with the help of different Cp values such that red areas being higher pressure and blue being lower pressure. In Subsonic Regime, bump original shows tendency of separation at supersonic mach. Bump softer has large regions of low pressure and severe swirls for subsonic speeds. This softer bump shows maximum separation at supersonic speed. It can be seen in the streamline figures in the results section above. The Blunt bump has same tendency as softer bump but its swirls are not too severe. The capacity to divert the streamlines smoothly is connected to how big swirls that arise. Thus, bump Smaller and Original has the smoothest and most effective diversion of the streamlines. Blunt bump is giving rise to swirls. This is because of the reason that it has very low high-pressure areas. As it is designed as blunter surface so its most of the pressure is distributed at the starting point.

Blunt bump is giving rise to swirls. This is because of the reason that it has very low high-pressure areas. As it is designed as blunter surface so its most of the pressure is distributed at the starting point. Smaller bump has the same geometry as original bump but its magnitude is lesser. Its streamlines show that they remain attached and surface of this bump does not give rise to severe swirls. This is because of the reason that it has smaller magnitude and also the high-pressure areas.

At supersonic regime high pressure area is increased decreasing the flow separation and turbulence [22]. But at the same time at the rear the low-pressure area can add to the turbulence in an original bump. Streamlines predict flow separation near rear along with few swirls [23]. For the blunt shaped bump as per streamlines it is clear that flow separation exists at both sub and supersonic speeds. Softer bump at supersonic regimes shows very high turbulence and swirls which can be associated to more low-pressure areas due to which the streamlines are not forced to remain attached to the surface which results in the flow separation [24] & subsequently turbulence.

From the mach contours we desire that flow is decreased after interacting the bump so the workload of the diffuser can be reduced thus Mach no of flow along the bump should decrease [25] and we have following observations from the results:-

• Increase of Mach at the top of the bumps.
• For Mach no >1 or for supersonic speed there is a non-attached oblique shock.

Therefore, bump must be placed relative to the intake duct so that this oblique shock wave is directed on the cowl lip of duct and shock on lip phenomenon is achieved [26]. As per table 2, the pressure recoveries have not shown significant difference at subsonic Mach. Bump smaller gives highest pressure recovery at 0.6 Mach. But there is not much difference in pressure recovery for all bumps at subsonic speed. When we reach transonic or supersonic Mach then this pressure recovery becomes more critical [27].

XI. CONCLUSION

A bump with smooth beginning and end gives better results as compared to blunter bump. Original bump gave better results than blunter bump because the blunt bump has more flow separation & shock induced separation as stronger shock wave is formed in case of blunter shape. Smaller and original bump gave similar pressure recoveries and it is proved that amplitude of bump has no significant effects at subsonic regimes. However, at supersonic regimes the higher amplitude of the bump in air intakes will cause higher pressure recoveries because of shock waves & results with smaller amplitudes can be improved by positioning them more into the air intakes. As we know that flow starts to separate after maximum amplitude of the bump so the position of bump plays important role. Thus, bump should be such that its maximum amplitude comes close to the cowl lip of intake duct, so that shock on lip condition is met.

CONFLICTS OF INTEREST

The authors declare that they have no conflicts of interest.

REFERENCES

[1] Seddon, J. and E. L. Goldsmith, *Intake aerodynamics*. Washington, D.C.: American Institute of Aeronautics & Astronautics, 1999.

[2] Sóbester, A., "Tradeoffs in jet inlet design: A historical perspective," *Journal of Aircraft*, vol. 44, no. 3, pp. 705–717, 2007. Available from: https://doi.org/10.2514/1.26830

[3] Javaid, M. T., Sajjad, U., ul Hassan, S. S., Nasir, S., Shahid, M. U., Ali, A., and Salamat, S., "Power enhancement of vertical axis wind turbine using optimum trapped vortex cavity," *Energy*, vol. 278, 127808, 2023. Available from: https://doi.org/10.1016/j.energy.2023.127808

[4] Nasir, S., Zainab, H., and Hussain, H. K., "Artificial-Intelligence Aerodynamics for Efficient Energy Systems: The Focus on Wind Turbines," *BULLET: Jurnal*

Multidisiplin Ilmu, vol. 3, no. 5, pp. 648–659, 2024. Available from: https://tinyurl.com/45u7m3xu

[5] ul Hassan, S. S., Javaid, M. T., Rauf, U., Nasir, S., Shahzad, A., and Salamat, S., "Systematic investigation of power enhancement of Vertical Axis Wind Turbines using bio-inspired leading-edge tubercles," *Energy*, vol. 270, 126978, 2023. Available from: https://doi.org/10.1016/j.energy.2023.126978

[6] Hoyle, N., Bressloff, N., and Keane, A., "Design optimization of an engine air intake," 2005. Available from: https://eprints.soton.ac.uk/41988/

[7] Valorani, M., et al., "Optimal supersonic intake design for air collection engines (ACE)," *Acta Astronautica*, vol. 45, no. 12, pp. 729–745, 1999. Available from: https://doi.org/10.1016/S0094-5765(99)00185-X

[8] Tahir, R. B., *Analysis of Shock Dynamics in Supersonic Intakes*, 2009. Available from: https://tinyurl.com/mrtday5c

[9] Cui, K., et al., "Conceptual design and aerodynamic evaluation of hypersonic airplane with double flanking air inlets," *Science China Technological Sciences*, vol. 56, no. 8, pp. 1980–1988, 2013. Available from: https://link.springer.com/article/10.1007/s11431-013-5288-0

[10] Raza, A., Farhan, S., Nasir, S., and Salamat, S., "Applicability of 3D printed fighter aircraft model for subsonic wind tunnel," in *2021 Int. Bhurban Conf. Applied Sciences and Technologies (IBCAST)*, pp. 730–735, 2021. Available from: https://ieeexplore.ieee.org/abstract/document/9393214

[11] Nasir, S., Javaid, M. T., Shahid, M. U., Raza, A., Siddiqui, W., and Salamat, S., "Applicability of Vortex Lattice Method and its Comparison with High Fidelity Tools," *Pakistan Journal of Engineering and Technology*, vol. 4, no. 1, pp. 207–211, 2021. Available from: https://doi.org/10.51846/vol4iss1pp207-211

[12] Shahid, M. U., Javaid, M. T., Nasir, S., Sajjad, U., Haider, F., ul Hassan, S. S., and Salamat, S., "Development and Fidelity Assessment of Potential Flow based Framework for Aerodynamic Modeling of High Lift Devices," *Pakistan Journal of Engineering and Technology*, vol. 5, no. 2, pp. 104–111, 2022. Available from: https://doi.org/10.51846/vol5iss2pp104-111

[13] Sahibzada, S., Malik, F. S., Nasir, S., and Lodhi, S. K., "AI-Augmented Turbulence and Aerodynamic Modelling: Accelerating High-Fidelity CFD Simulations with Physics-informed Neural Networks," *International Journal of Innovative Research in Computer Science and Technology*, vol. 13, no. 1, pp. 91–97, 2025. Available from: https://tinyurl.com/bdcrw2ak

[14] Sahibzada, S., Malik, F. S., Nasir, S., and Lodhi, S. K., "Generative AI Driven Aerodynamic Shape Optimization: A Neural Network-Based Framework for Enhancing Performance and Efficiency," *International Journal of Innovative Research in Computer Science and Technology*, vol. 13, no. 1, pp. 98–105, 2025. Available from: https://tinyurl.com/57frh49x

[15] Nasir, S., Sahibzada, S., and Malik, F. S., "Adjoint-Based Optimization for Enhanced Aerodynamic Performance Using Multi-Parameterization Techniques," *International Journal of Innovative Research in Computer Science and Technology*, vol. 13, no. 2, 2025. Available from: https://tinyurl.com/2u9jwejw

[16] Ahmad, M., et al., "Experimental Investigation of Wing Accuracy Quantification using Point Cloud and Surface Deviation," *Pakistan Journal of Engineering and Technology*, vol. 4, no. 2, pp. 13–20, 2021. Available from: https://doi.org/10.51846/vol4iss2pp13-20

[17] Creta, F. and Valorani, M., "Optimal Shape Design of Supersonic, Mixed-Compression, Fixed-Geometry Air Intakes for SSTO Mission Profiles," in *38th AIAA/ASME/SAE/ASEE Joint Propulsion Conf. & Exhibit*, 2002. Available from: https://doi.org/10.2514/6.2002-4133

[18] Khan, O. and Masud, J., "Evaluating an Experimental Streamlined Fairing for a Diverter Less Supersonic Inlet (DSI) Equipped Aircraft," 2016. Available from: https://doi.org/10.2514/6.2016-1566

[19] Neale, M. and Lamb, P., *Tests with a variable ramp intake having combined external/internal compression and a design Mach number of 2.2*. London: HM Stationery Office, 1965. Available from: https://tinyurl.com/nheujxur

[20] Fisher, S., Neale, M., and Brooks, A., *On the sub-critical stability of variable ramp intakes at mach numbers around 2*. Citeseer, 1970. Available from: https://reports.aerade.cranfield.ac.uk/handle/1826.2/2987

[21] Kim, S. D. and Song, D. J., "Numerical study on performance of supersonic inlets with various three-dimensional bumps," *Journal of Mechanical Science and Technology*, vol. 22, no. 8, pp. 1640–1647, 2008. Available from: https://link.springer.com/article/10.1007/s12206-008-0503-9

[22] Svensson, M., "A CFD Investigation of a Generic Bump and its Application to a Diverterless Supersonic Inlet," 2008.

[23] Masud, J. and Akram, F., "Flow field and performance analysis of an integrated diverterless supersonic inlet," *Aeronautical Journal*, vol. 115, no. 1170, p. 471, 2011. Available from: https://doi.org/10.1017/S0001924000006114

[24] Watanabe, Y. and Murakami, A., "Control of supersonic inlet with variable ramp," in *Proc. ICAS*, 2006. Available from: https://tinyurl.com/sac5wk4s

[25] Ferguson, F., Dasque, N., and Dhanasar, M., "Waverider Design and Analysis," *Aeronautical Journal*, 2015. Available from: https://doi.org/10.2514/6.2015-3508

[26] Romander, E., Norman, T. R., and Chang, I.-C., "Correlating CFD simulation with wind tunnel test for the full-scale UH-60A airloads rotor," in *Proc. 67th American Helicopter Society International Annual Forum*, 2011. Available from: https://ntrs.nasa.gov/citations/20110014374

[27] Alexander, D., Jenkins, H., and Jones, P., "A comparison of wind tunnel and CFD methods applied to natural ventilation design," in *Proceedings of Building Simulation*, 1997. Available from: https://tinyurl.com/5yybbk2d